BCSJ

Nucleophilic Attack of R-lithium at Tetrahedral Silicon in Alkoxysilanes. An Alternate Mechanism

Joseph C. Furgal[1] **and Richard M. Laine***[2,3]

[1]Department of Chemistry, University of Michigan, Ann Arbor, Michigan 48109-2136, USA

[2]Department of Materials Science and Engineering, University of Michigan, Ann Arbor, Michigan 48109-2136, USA

[3]Department of Macromolecular Science and Engineering, University of Michigan, Ann Arbor, Michigan 48109-2136, USA

E-mail: talsdad@umich.edu

Received: January 31, 2016; Accepted: February 22, 2016; Web Released: February 29, 2016

Richard M. Laine

Richard M. Laine received his Ph.D. in Chemistry (1973) from the University of Southern California supervised by Professor Robert Bau. He did postdoctoral work before moving to Stanford Research Institute (1976–87). He moved to the Dept of Materials Science and Engineering, University of Michigan in 1990 and became a full professor in 1995. Most recently he served as director of Macromolecular Science and Engineering Center (2006–2015). He is an ACS Fellow (2015) and an International Fellow of the Society for Polymer Science of Japan (2013). His research interests include the synthesis and processing of organic/inorganic hybrid materials.

Abstract

The currently accepted mechanism for nucleophilic attack at silicon in tetraalkoxysilanes, e.g. $Si(OEt)_4$ is suggested to involve formation of penta- and then hexacoordinated intermediates as supported by the apparent exclusive formation of R_3SiOR' and R_4Si from nucleophilic attack by RLi and RMgX. Our recent discovery of a direct route from biogenic silica to tetraalkoxyspirosiloxanes prompted us to revisit this reaction as a potential route to diverse silicon-containing species with single Si–C bonds as early studies demonstrate that spirosiloxanes form quite stable pentacoordinated alkoxysilane compounds. As anticipated, Si(2-methyl-2,4-pentanediolato)$_2$ (SP) reacts with RLi (R = Ph, anthracene, phenylacetylene, etc.) at −78 °C to form pentacoordinated Si, e.g. LiPhSP equilibrates with the starting reagents even at 3:1 ratios of PhLi:SP with no evidence for formation of hexacoordinated species by mass spectral, NMR and quenching studies. Thus, quenching with MeI or Me_3SiCl allows isolation of monosubstituted products from RLi:SP; $RSi(OR')_3$ including some ring-opened oligomers. Comparative studies of reactions of PhLi with $Si(OEt)_4$ allows isolation of mono- and disubstituted products again even at 1:1 ratios of PhLi:$Si(OEt)_4$. However, on standing at −78 °C for long periods of time or on warming to 0 °C, the primary product for both reactions is Ph_4Si *even with 0.5 equivalents of PhLi*. At reaction temperatures ≥0 °C the primary product is again Ph_4Si. These results suggest that hexacoordinated intermediates are not part of the substitution mechanism and may suggest that the higher-substituted compounds arise from disproportionation processes. We also briefly describe the conversion of anthracenylSP and 9,9-dimethylfluoreneSP to silsesquioxanes.

Introduction

Silicon chemistry is dominated by compounds made starting from the products of the direct process, reaction (1).[1] Other products can be made from $PhSiCl_3$ available via reaction (2).[2] Finally, hydrosilylation as exemplified by reaction (3), provides access to other types of monofunctional silanes.[3,4]

$$Si_{met} + MeCl \xrightarrow{Cu/Sn\ cat/300^\circ C} MeSiCl_3 + Me_2SiCl_2 + MeHSiCl_2\ (\text{polysiloxane precursors}) \quad (1)$$

$$Ph\text{-}H + SiCl_4 \xrightarrow{BCl_3\ cat/350^\circ C} PhSiCl_3 \quad (2)$$

$$HSiCl_3 + CH_2{=}CH\text{-}R \xrightarrow{cat} R\text{-}CH_2CH_2SiCl_3 \quad (3)$$

However, if one wants to make organosilicon compounds starting from organic compounds that do not contain an accessible double bond or compounds without phenyl or methyl groups, very few synthetic avenues remain. These typically involve reactions of nucleophiles with chloro- or alkoxysilanes as illustrated in reactions (4) and (5).

$$SiCl_4 + RLi\ (RMgBr) \xrightarrow{solvent} R_{4-x}SiCl_x + (x = 0\text{–}3) + LiCl\ (MgBrCl) \quad (4)$$

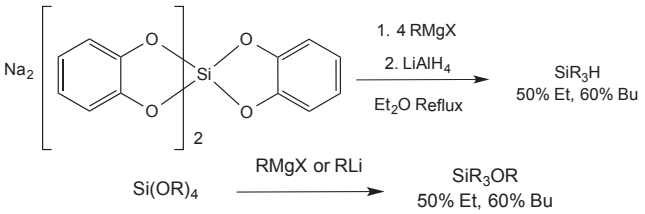

Scheme 1. Typical reactions of triscatecholatosilicate or tetralkoxysilanes with Grignard and lithium reagents.[5–16]

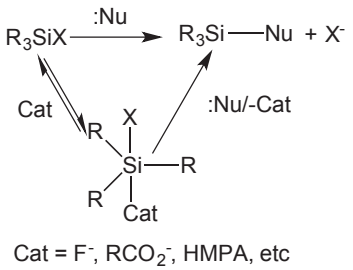

Scheme 2. Proposed mechanism for nucleophilic substitution at Si via pentacoordinate intermediates.[15,16]

$$\mathrm{Si(OR)_4 + R'Li\ (RMgBr)} \xrightarrow{\text{solvent}} \mathrm{R'_{4-}}_x\mathrm{Si(OR)}_x\ (x = 0\text{–}3) + \mathrm{LiOR\ (MgBrOR)} \quad (5)$$

Reaction (4) proceeds reasonably well but one must contend with chlorosilanes before and after reaction and their hydrolysis products, which require extra care and often afford unwanted complications including the formation of intractable polymers. Consequently, multiple groups have explored nucleophilic attack at $Si(OEt)_4$ (TEOS) in particular using strong nucleophiles, however no others have targeted the synthesis of silsesquioxane precursors [$RSi(OR')_3$] and more importantly difunctional siloxanes [$–R_2SiO–$ or $R_1R_2SiO–$] where R is not methyl.

Reaction (5) also suffers from an important complication because nucleophilic substitution often does not stop at the monofunctional silane but rather commonly continues to the tri- and tetrafunctional products even when the alkoxysilane is used in excess, as suggested in Scheme 1.[5–11] Thus, nucleophilic attack at tetrahedral alkoxysilanes differs considerably from that of carbon-containing compounds.

This surprising result has prompted multiple studies on nucleophilic attack at tetrahedral silicon. Extensive studies by the Corriu group provide considerable evidence that nucleophilic attack occurs much faster at penta- and hexacoordinated rather than tetrahedral silanes.[12–16] They have proposed a general mechanism as illustrated in Scheme 2.[15,16] Here F^- or RCO_2^- would be a catalyst for reactions not involving Grignard or Li reagents.

This mechanism seems to provide an explanation for many of the results reported to date.[5–11] Corriu et al. argue that in the absence of catalyst, the nucleophile takes the position "Cat" in Scheme 2; thus, double and triple functionalization can be expected. Many of the Corriu et al. studies were run in ether at or near reflux temperatures (≈30 °C).

Tour et al. demonstrated that it was possible to get two of the same R groups to add to Si using alkyl-/aryllithium reagents and thereafter add a different R′Li group to produce $R_2R'SiOEt$.[7] They could never obtain $RR'Si(OR)_2$, again supporting the likelihood that pentacoordinate species react faster than tetracoordinate ones. Although their reactions were initiated at −78 °C, they were allowed to warm to room temperature prior to quenching with water.

In relatively recent work, Manoso et al.[10] and later Jung et al.[11] found that −78 °C aryl lithium and −30 °C Grignard reagents react with TEOS or $Si(OMe)_4$ (TMOS) to produce monofunctional alkoxysilanes, $RSi(OR)_3$. In these studies it was found that low-temperature reaction conditions, excess TEOS (>2 equiv) and low-temperature quenching are key aspects in obtaining monofunctional products. Manoso et al. also found that nucleophilic substitution reactions worked best with electron poor as opposed to electron-rich aryl reagents, which are more reactive and tended to form R_2Si, R_3Si, and R_4Si as found by Corriu. They also reported that reaction time has little influence on reaction products and yields, regardless of temperature and RLi(MgBr):TEOS stoichiometries (e.g. even at 1:3 ratios) always providing some quantities of di- and trialkoxysilanes. In contrast to the work of Tour, these researchers quenched with water at −78 °C prior to allowing the reactions to warm to room temperature. It appears that warming before quenching makes quite a difference in the spectrum of products.

Our interest in this area is driven by the need to develop new ways to make arylsilsesquioxanes given our extensive work on their properties.[17–22] We have previously reported the facile synthesis of pentacoordinated spirosilicates from any silica source in ethylene glycol.[23] The glycolato silicate of reaction (6) can be isolated in quantitative yield and appears to be quite stable suggesting that spirosiloxanes might be better candidates for stabilizing the monofunctionalized species as suggested by reaction (7).

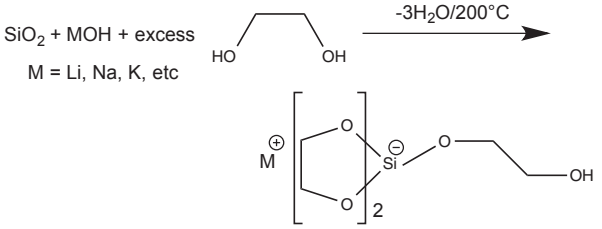

(6)[20]

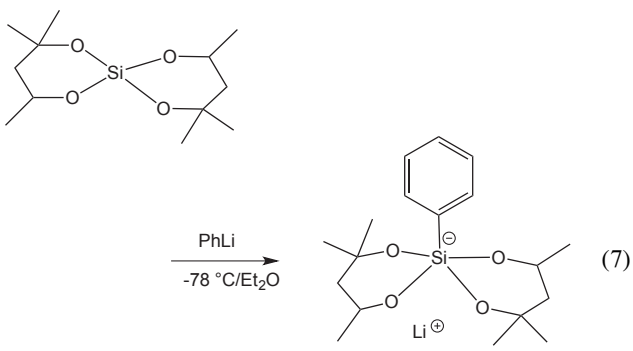

(7)

Thus, our recent discovery of the direct depolymerization of biogenic silica sources such as rice hull ash (RHA) to produce spirosiloxanes per reactions (8) and (9) offered an exceptional opportunity to develop greener routes to special mono- and difunctional silicon-containing compounds.[24] We report here our first successful efforts to develop such routes.

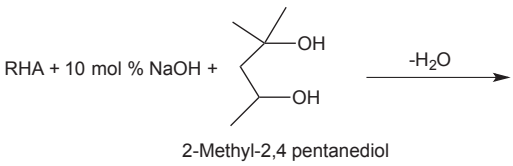

2-Methyl-2,4 pentanediol

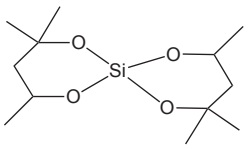

(8)

I

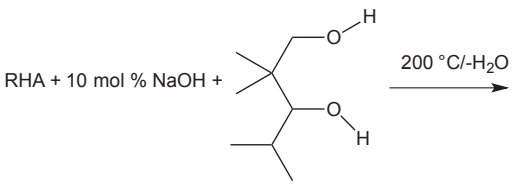

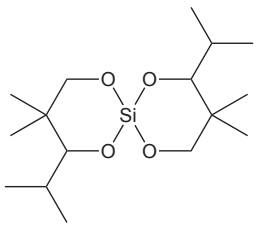

(9)

Experimental

Materials. Chemicals and solvents were obtained from commercial suppliers and used without further purification, unless otherwise indicated. Spirosiloxane **I** was synthesized as described elsewhere.[24] All other chemicals were purchased from Fisher Scientific or Aldrich Chemical and used as received.

Spirosiloxane: R-lithium Reaction. To a flame dried and argon purged 100 mL Schlenk flask was added 2.5 g (10 mmol) of spirosiloxane **I** and a magnetic stir bar. The flask was then evacuated under vacuum 3 times and purged with argon. The flask was then cooled to either −40 [dry ice/ethylene glycol (0.6):ethanol (0.4)] or −78 °C (dry ice/acetone bath for 10 min under argon. Then 75 mL of dry argon purged diethyl ether was added to the reaction and allowed to cool for another 10 min. Then 10 mmol of R-lithium solution in diethylether was added dropwise by syringe to the reaction mixture, at which time the reaction became a yellow color. The reaction was run till the yellow color subsided and was then quenched with excess Me_3SiCl or MeI and allowed to stir cold for >30 min before warming up. The reaction was then worked up by a quick water wash (2 times) to remove salts and then dried over $MgSO_4$. The reaction was then filtered through Celite to remove salts and solvent removed in vacuo. A clear semi-viscous oil was obtained. Further purification on select samples was achieved by bulb-to-bulb distillation under reduced pressure. Characterization is given in tabular form in the text. Reaction conversions were calculated by integrating the NMR peaks for each species and determining the ratio of the desired product versus the total area.

Spirosiloxane: R-arylbromide Reaction. To a flame dried, 3 times evacuated and argon purged 25 mL Schlenk flask was added 4.6 mmol of aryl bromide (2-bromo-9,9-dimethylfluorene, 9-bromoanthracene, and 1-bromo-4-methylnaphthalene) and a magnetic stir bar. The flask was then cooled to −78 °C (dry ice/acetone bath) for 10 min under argon (room temperature for phenylacetylide). Then 10 mL of dry argon purged diethyl ether was added to the reaction and allowed to cool for another 10 min. This was followed by 2.2 mL (5.5 mmol) of *n*-butyllithium solution in diethyl ether. The reaction was allowed to stir for 30 min to complete the halide-exchange reaction, at which time the reactions turned a yellow color and salt precipitates formed. Then 1 g (3.8 mmol) of spirosiloxane **I** dissolved in 5 mL of cooled dry argon purged diethyl ether was added by syringe to the reaction mixture and allowed to stir for an additional 2 h. The reaction was run till the yellow color subsided and was then quenched with excess Me_3SiCl and allowed to stir cold for >30 min before warming up. The reaction was then worked up by a quick water wash (2 times) to remove salts and then dried over $MgSO_4$. The reaction was then filtered through Celite to remove salts and solvent removed in vacuo. Yellow-orange viscous oils were obtained. Characterization is given in tabular form in the text.

Tetraethoxysilane: PhLi Reaction. To a flame dried, 3 times evacuated and argon purged 25 mL Schlenk flask was added 1.07 mL (4.8 mmol) of TEOS and a magnetic stir bar. The flask was then cooled to either −40 [dry ice/ethylene glycol (0.6):ethanol (0.4)] or −78 °C (dry ice/acetone) bath for 10 min under argon. Then 15 mL of dry argon purged diethyl ether was added to the reaction and allowed to cool for another 10 min. Then 4.8 mmol of a PhLi solution was added dropwise by syringe to the reaction mixture, which became yellow in color. The reaction was run till the yellow color subsided and was then quenched with excess Me_3SiCl or MeI and allowed to stir cold for >30 min before warming up. The reaction was then worked up by a quick water wash (2 times) to remove salts and then dried over $MgSO_4$. The mixture was then filtered and the solvent removed in vacuo. A clear semi-viscous oil was obtained. Characterization is given in tabular form in the text.

Silsesquioxane Synthesis (Ph-Example).[21,22] Briefly, 150 mg of oligomeric monoPh-**I** were added to a 50 mL round bottom flask with a magnetic stirrer. Then 30 mL of CH_2Cl_2 was added to the reaction, followed by 20 µL of water and 25 µL of 1 M TBAF solution in THF. The reaction was left to stir for 16 h, and was then quenched with 50 mg of $CaCl_2$ to remove fluoride. The reaction was then filtered through Celite, and solvent removed in vacuo. The product was then dissolved in a small amount of CH_2Cl_2 and precipitated into methanol to remove partial cage by-products. The precipitate was then filtered, giving 62 mg of isolated PhSQ products in a mixture of cage sizes (T_8, T_{10}, and T_{12}). Other cages were synthesized in a similar manner. Characterization data is given in the text.

Analyical Methods. NMR Analyses: ^1H and ^{29}Si NMR were measured in diethyl ether or chloroform-*d* with TMS (0.00 ppm) as the internal reference on a Varian VNMRS 500 spectrometer. ^1H NMR spectra were collected at 500 MHz using a 7998.4 Hz spectral width, a pulse width of 45°, relaxation delay of 0.5 s, 65K data points. ^{13}C NMR spectra were collected at 100 MHz using a 25000 Hz spectral width, a pulse width of 40°, relaxation delay of 1.5 s, and 75K data points. ^{29}Si NMR spectra were collected at 99.35 MHz using a 4960 Hz spectral width, a pulse width of 7°, a relaxation delay of 15 s, and 4K data points.

Mass Spectroscopy (MS): Electron impact (EI) analyses were conducted using a VG 70-250-S magnetic sector instru-

ment (Waters) by electron impact ionization (EI). The instrument was calibrated with perfluorokerosene-H. The samples were run in EI mode at 70 eV electron energy with an ion source temperature of 240 °C. The mass range was scanned from m/z 1000 to 35. High-resolution mass spectrometry (HRMS) analysis was conducted on the same instrument.

Electrospray ionization (ESI) was performed on an Agilent Q-TOF system with a dual ESI ion source. The mobile phase consisted of a 9:1 mixture of acetonitrile:water with 0.1% formic acid. Lockmass correction was used to obtain mass accuracy.

Matrix-assisted laser desorption ionization time-of-flight (MALDI-TOF) was performed on a Micromass TofSpec-2E equipped with a 337 nm nitrogen laser in positive-ion reflectron mode using poly(ethylene glycol) as calibration standard, dithranol as matrix, and $AgNO_3$ as ion source. Sample was prepared by mixing solution of 5 parts matrix (10 mg mL^{-1} in THF), 5 parts sample (1 mg mL^{-1} in THF), and 1 part of $AgNO_3$ (2.5 mg mL^{-1} in water) and then spotting the mixture on a stainless steel target plate.

Gel Permeation Chromatography (GPC): GPC analyses were run on a Waters 440 system equipped with Waters Styragel columns (7.8 × 300, HT 0.5, 2, 3, 4) with a Waters 2410 refractometer for detection, with THF as the solvent. The system was calibrated using polystyrene standards and toluene as reference. Analyses were performed using PL Caliber 7.04 software (Polymer Labs, Shropshire UK).

Fourier Transform Infrared Spectroscopy (FTIR): Diffuse reflectance Fourier transform (DRIFT) spectra were recorded on a Nicolet 6700 Series FTIR spectrometer (Thermo Fisher Scientific, Inc., Madison, WI). Optical grade, random cuttings of KBr (International Crystal Laboratories, Garfield, NJ) were ground (400 mg) with 5 mg of sample to be analyzed. For DRIFT analyses, samples were packed and smoothed off to ensure little scattering. The FTIR sample chamber was flushed continuously with N_2 prior to data acquisition in the range 4000–400 cm^{-1} with a precision of ±4 cm^{-1}.

Results and Discussion

In the following sections we first discuss the substitution reactions of PhLi with **I**, and analyze the effects of temperature and quenching on the final structures. This is followed by studies on the stoichiometric reactions of various other RLi reagents (i.e. phenylacetylenyl, anthracenyl, etc.) with **I** and characterization studies. The reactions of PhLi with tetraethoxysilane (TEOS) are also discussed. Lastly, several examples are given using R-**I** to synthesize novel silsesquioxanes by fluoride catalyzed cage formation.

Reactions with Spirosiloxane I. Our first steps in these efforts were to extend the work of Manoso et al. and Jung et al. to our system to compare the reactions of TEOS with those of **I** produced per reaction (8).[10,11] As such, studies were initiated using *stoichiometric* PhLi/Et_2O/−78 °C to arylate **I** resulting in facile formation of monosubstituted Ph**I**Li (Reaction 10). Figure 1 presents the MALDI-TOF spectrum taken by spotting the −78 °C unquenched reaction mixture directly on a sample plate just prior to analysis.

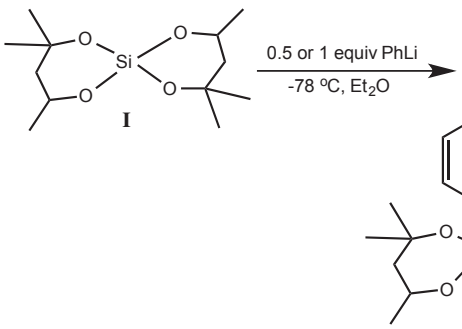

(10)

In contrast, if the above reaction of **I** with PhLi (1:1 ratio) is allowed to warm to ambient without quenching then a quite different product appears, which precipitates out of diethyl ether allowing easy separation from remaining **I**. The ^{29}Si NMR (Figure 2) of this product gives a single peak at $\delta = -14.4$ ppm, the literature value,[25] typical for tetraarylsilanes. The EI-MS (Figure S1) provides further evidence showing the tetraphenyl product peak at 336.0 m/z. If the same reaction is run with a ratio of 0.5:1 similar peak distributions are observed in the EI-MS mass spec (Figure S2). This product distribution is truly unique, since it tells us something about the reaction itself. Since only monophenyl products are observed at low temperature (Figure 1), it suggests that PhLi reacts with **I** to form a pentacoordinated species, which then transfers the phenyls to other similar species multiple times until Ph_4Si forms as the final product. Corriu et al. report that reacting hexacoordinated catecholato spirosiloxanes with PhMgBr at 35 °C (Scheme **I**)

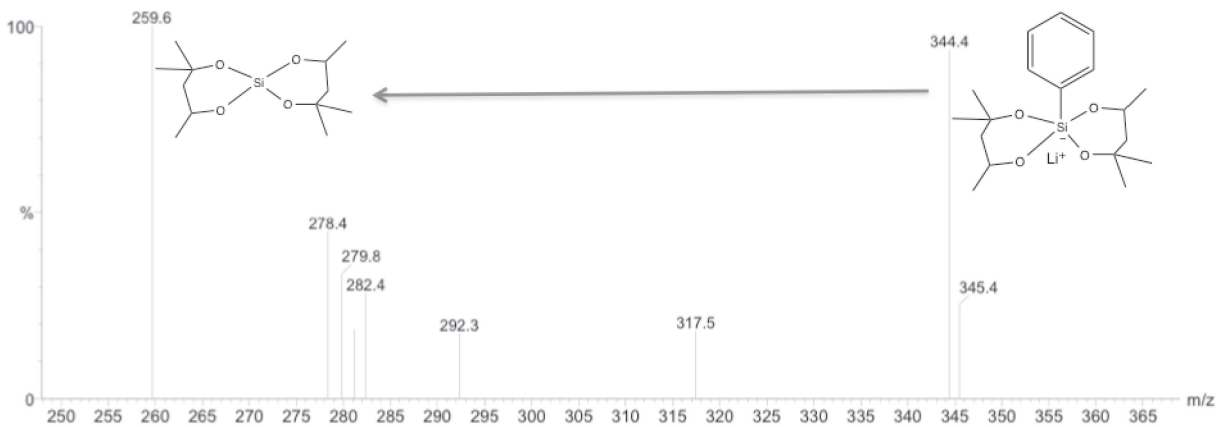

Figure 1. MALDI-TOF of 1:1 spirosiloxane (**I**):PhLi (−78 °C), $m/z \approx 344.4$ is the parent ion for LiPhSi(2-methyl-2,4-diolato)$_2$, which loses PhLi to give **I** at $m/z = 259$.

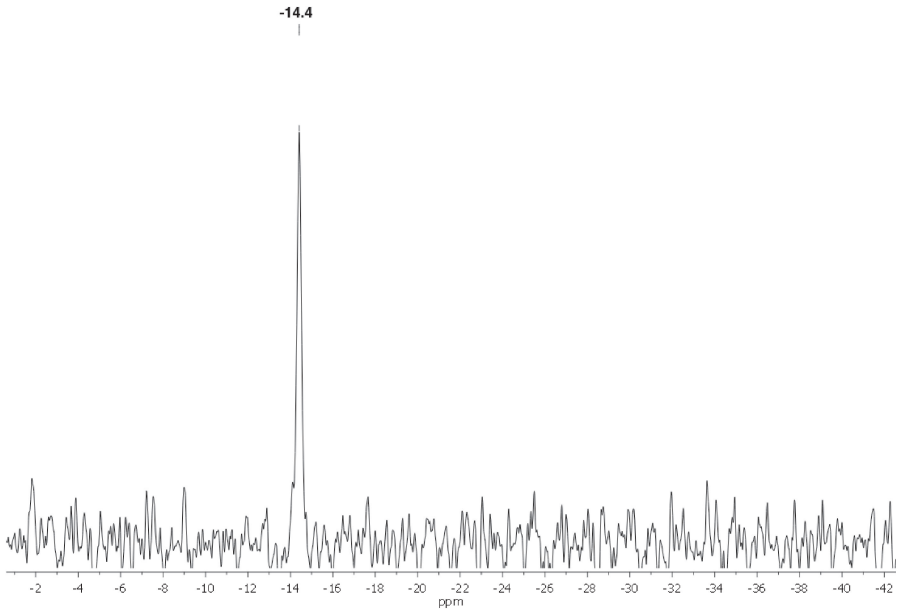

Figure 2. ^{29}Si NMR of synthesized tetraphenylsilane, −14.4 ppm, isolated from a 1:1 PhLi:**I** reaction run at −78 °C then warmed to room temperature without quenching, and then rinsed with diethyl ether to remove excess **I**.

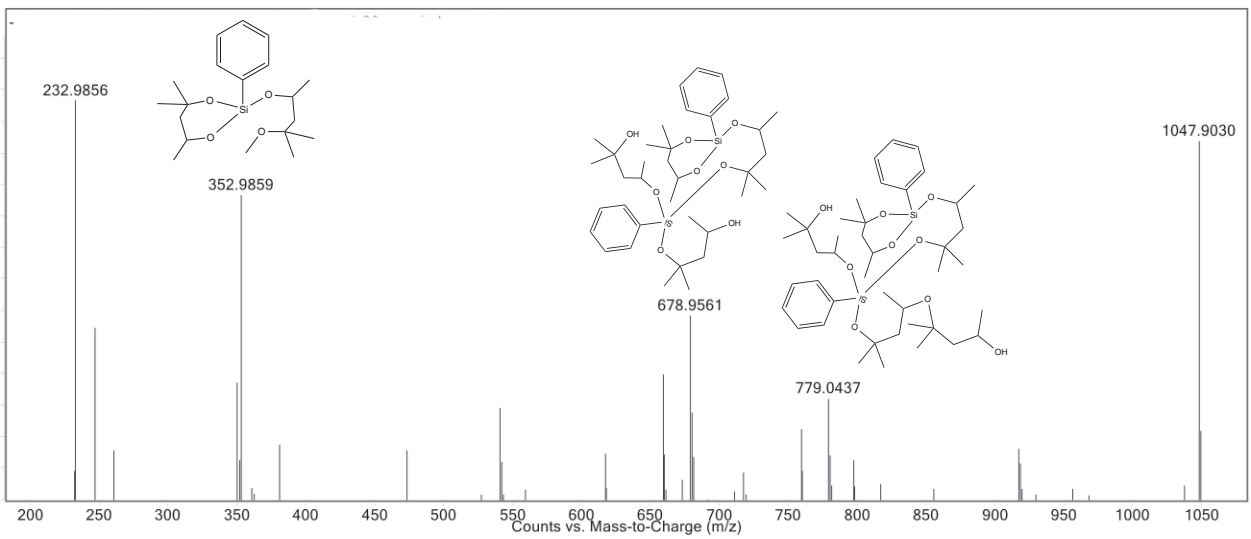

Figure 3. Negative ion ESI mass spectrum of 1:1 PhLi:**I** after quenching with MeI.

gives only Ph_4Si.[11,12,21,26,27] It seems plausible to suggest that these reactions occur via at least a heptacoordinated transition state rather than a penta- or hexacoordinated one. Running reactions at low temperatures and quenching with an electrophile before warming, circumvents this reaction pathway, see below.

Quenching the 1:1 PhLi:**I** reaction with MeI at −78 °C results in products that include ring-opened oligomers per the Figure 3 negative ion ESI-MS. The 352.9 m/z peak is the targeted quenched product **II** (Reaction 11), while the other peaks can be ascribed to ring-opened products with structures suggested in Figure 3. By-products of the substitution reaction such as dimer **III** are also observed in EI-MS at 457.9 m/z (Figure S3).

The Figure 4 ^{29}Si NMR shows product peaks at −57 ppm likely corresponding to $PhSi(OR)_3$ [$PhSi(OEt)_3$, Table 1] and at −63 to −67 ppm likely peaks from dimeric/oligomeric species containing Si–O–Si linkages (i.e., $[Ph(RO)_2Si–O–Si(OR)_2Ph]$) based on their structural similarity to T_1 species observed in the synthesis of silsesquioxanes.[28,29] The peaks upfield correspond to $Si(OR)_4$ species, including residual **I**. Table 1 shows literature values for ^{29}Si NMR of various alkoxysilanes.

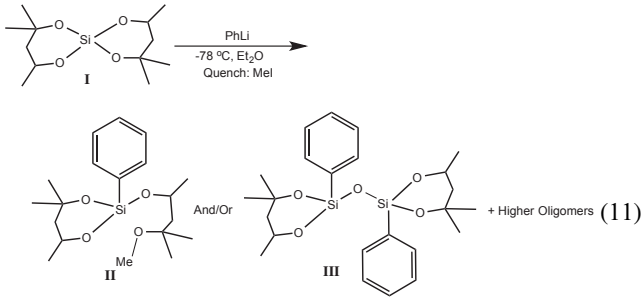

(11)

A small peak appears at −30 ppm that likely corresponds to $Ph_2Si(OR)_2$ [$Ph_2Si(OEt)_2$ in Table 1]. Note that even at a 1:1

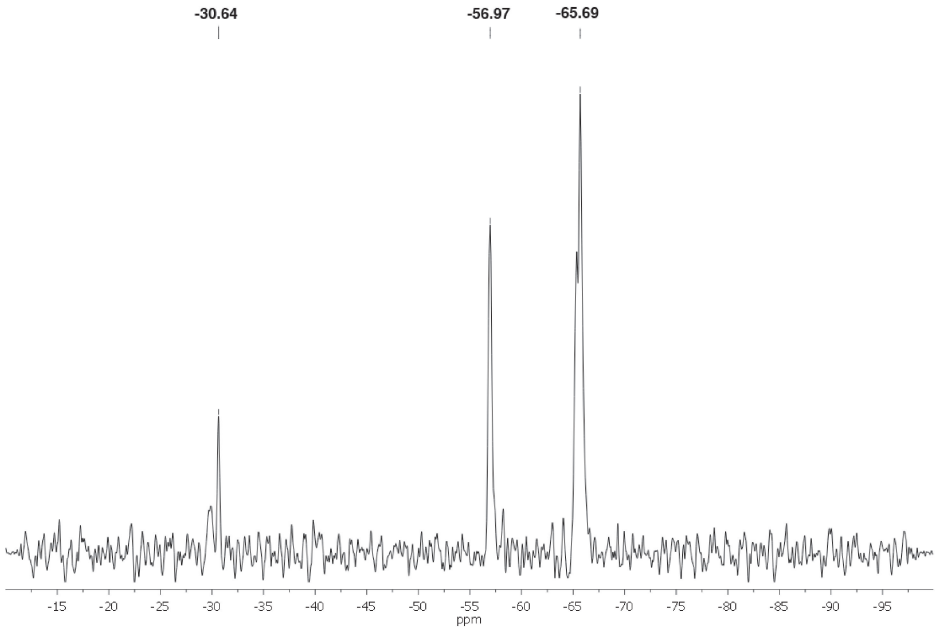

Figure 4. ^{29}Si NMR spectrum of the MeI quenched −78 °C 1:1 PhLi:**I** of Figure 2.

Table 1. Literature ^{29}Si NMR chemical shifts of selected alkoxysilanes in $CDCl_3$[30]

Formula	^{29}Si NMR/ppm
Ph_4Si[27]	−14.0
Me_3SiOEt	14.5
$Me_2Si(OEt)_2$	−4.3
$Ph_2Si(OEt)_2$	−32.4
$MeSi(OEt)_3$	−43.3
$MeSi(OPr)_3$	−43.3
$EtSi(OEt)_3$	−44.6
$CH_2{=}CHSi(OEt)_3$	−58.7
$CH{\equiv}CSi(OEt)_3$	−74.7
$PhSi(OEt)_3$	−57.9
4-$MePhSi(OEt)_3$	−57.2
$Ph(OEt)_2SiOSi(EtO)_2Ph$[28,29]	−64.9

reaction ratio, small quantities of unreacted **I** remain. This is more prevalent in the TMSCl quenched samples discussed below. Though Manoso et al. and Jung et al. both found good yields (>50%) by quenching the TEOS systems with water; we find that H_2O quenching of nucleophilic reactions of **I** give many ring-opened by-products, likely due to the formation of hydroxide ions. To overcome these drawbacks, our quenching studies used TMSCl and MeI, see reaction (12) and Scheme 3. Table 2 summarizes the PhLi:**I** reaction conditions, % conversions, ^{29}Si NMR, and MS results.

TMSCl quenching is complete in half the time needed for MeI (<30 min) vs. MeI (>1 h). Figure 5 provides an EI-MS for a 3 h reaction quenched with TMSCl. The desired quenched product appears at 410 m/z (**IV**) with the representative ^{29}Si NMR seen in Figure 6. The peak at −58 ppm corresponds to a $PhSi(OR)_3$ product (**IV**) per Table 1, the peak at −82 ppm is remaining **I** and the peak at −4.8 ppm is TMS-benzene, from quenching PhLi. A TMS–O– signal would appear at ca. 18 ppm but is not seen.

To examine the influence of reaction times; we ran 1:1 PhLi:**I** reactions for 3, 4.5, and 6 h. Figure S4 shows the GPC of this set of reactions with similar peak retention times and shapes for the first two samples, while the 6 h reaction shows a broader peak, perhaps indicative of more extensive ring-opening polymerization.

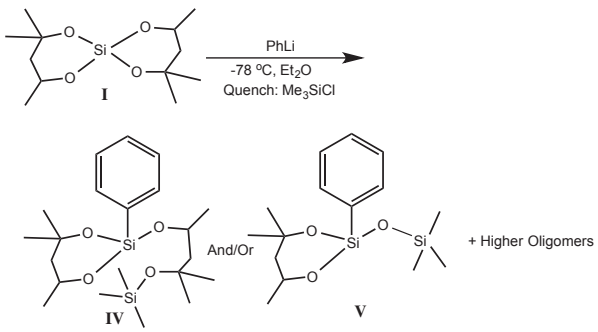

(12)

Mass spectral analysis reveals two new peaks at 310 m/z (**V**, –Me peak at 295 m/z) and 357 m/z (high-resolution mass spectral analysis indicates a formula of $C_{15}H_{25}Si_2O_6$, however we are unable to assign a structure for this formula). The 357 m/z peak is also more intense after 6 h vs. the 4.5 h reaction. Figure 7 shows an exemplary EI-MS of the 4.5 h sample. The Figure 8 ^{29}Si NMR for the 4.5 h reaction presents strong peaks in the ca. −65 ppm region, suggesting oligomers similar to those found in the MeI quenching studies.

One possible explanation for the formation of **V** and the Si–O–Si linkages in oligomeric derivatives is through cleavage of C–O bonds on the diol subunits during quenching. This would produce Si–O^- or Si–OH, which thereafter reacts with an electrophile (TMS), and a chloro-substituted alkyl (from diol) is made as a by-product. Such reactions are observed for Michaelis–Arbuzov rearrangement reactions with phosphorus,[31] and as suggested in the synthesis of phenylsilsesquioxane from phenyltrichlorosilane.[32]

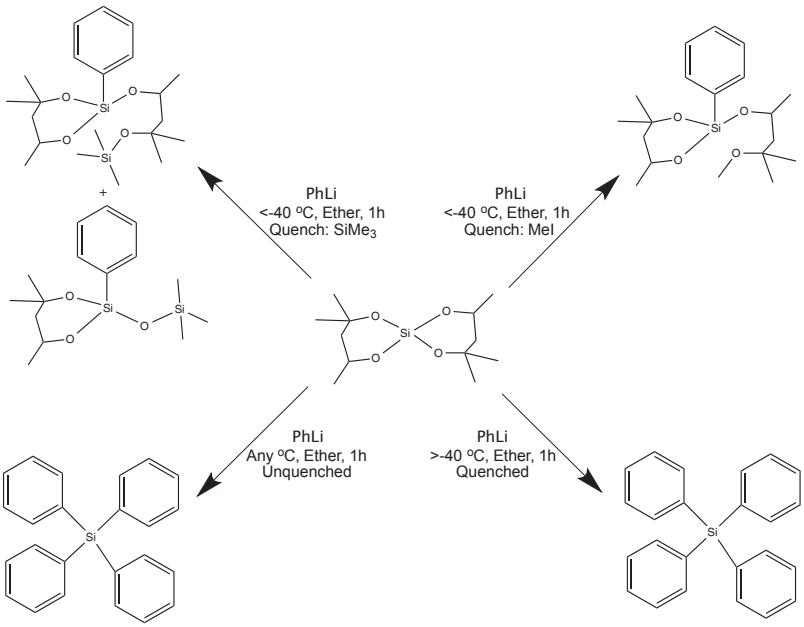

Scheme 3. Example reaction conditions for the substitution of **I** with PhLi and their dominant substituted products from Table 2.

Table 2. Reaction conditions and observed characterization data for PhenylLi reactions with spirosiloxane, all reactions were conducted at −78 °C for 2 h (**I**: spirosiloxane)

Rxn ratio	Structures	Observed MS (m/z)	^{29}Si NMR /ppm	Quenched	Conversion[a]/% (^{29}Si NMR)
1:1 PhLi:**I** (−78 °C)	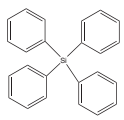	336.0	−14.4	No	100
1:1 PhLi:**I** (−78 °C)	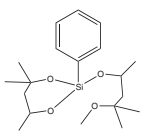	352.9	−57.0	MeI	100 Ph_1**I** + Ph*Si*(O)$_x$
	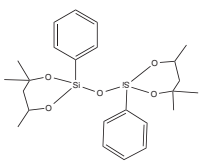	457.9	−65		
	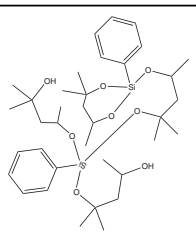	678.9	ca. (−65)		
	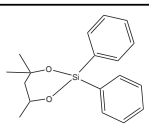	N/A	−30.6		
	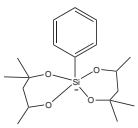	344.4	N/A		

Continued on next page.

Continued.

Rxn ratio	Structures	Observed MS (m/z)	^{29}Si NMR /ppm	Quenched	Conversion[a]/% (^{29}Si NMR)
0.5:1 PhLi:**I** (−78 °C)	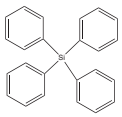	336.1	N/A	MeI	N/A
	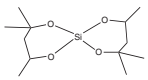	260.1, 243.2 ($M^+ - Me$)			
	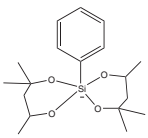	337.1			
0.5:1 PhLi:**I** (−78 °C)	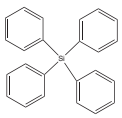	336.1	N/A	No	N/A
	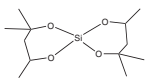	260.1, 243.2 ($M^+ - Me$)			
0.6:1 PhLi:**I** (−40 °C)	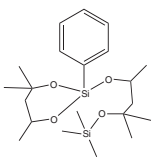	410.1	18.1, −58.9	Me_3SiCl	36 Ph_1**I** + Ph*Si*(O)$_x$
	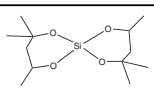	260.1	−82.1		
	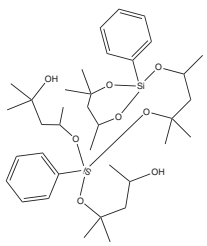	N/A	−64 to −68		
1:1 PhLi:**I** (−40 °C, 30 min)	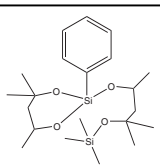	410.1	−58.9	Me_3SiCl	46 Ph_1**I** + Ph*Si*(O)$_x$
	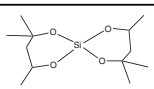	260.1	−82.1		
	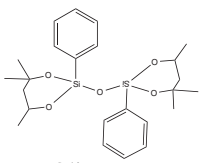 Oligomers	N/A	ca. −64		
	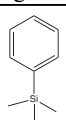	N/A	−4.8		

Continued on next page.

Continued.

Rxn ratio	Structures	Observed MS (m/z)	^{29}Si NMR /ppm	Quenched	Conversion[a]/% (^{29}Si NMR)
1:1 PhLi:**I** (−78 °C, 3 h)	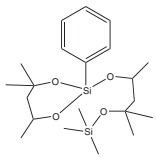	410.1	18, −57	Me_3SiCl	47 Ph_1**I** + Ph*Si*(O)$_x$
	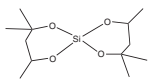	259.1	−82		
	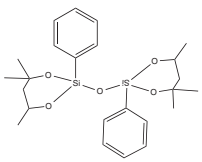 Oligomers	N/A	ca. −65		
	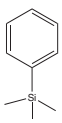	N/A	−4.8		
1:1 PhLi:**I** (−78 °C, 4.5 h)	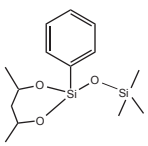	310.1	9.2, −65	Me_3SiCl	88 Ph*Si*(O)$_x$
	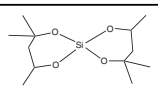	245.1 (M^+ − Me)	−82		
	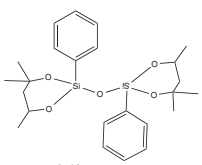 Oligomers	N/A	−66, −69		
	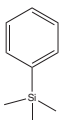	N/A	−4.8		

Continued on next page.

A general observation that can be made from all of our studies (see SI for more details) is that there is little change in the product distribution and starting materials no matter what reaction conditions are chosen (see below). These results suggest equilibration between starting materials and products, is the first step in nucleophilic attack and a significant barrier exists to a second such attack, contrasting greatly with the work and mechanisms of reaction suggested by Tour et al., Corriu et al., Manoso et al., and Jung et al.[7,10–12]

In all reaction studies done at −40 °C or below, 1:1 PhLi:**I** reactions almost always contain **I** in a nearly 1:1 Ph**I**:**I** ratio by ^{29}Si NMR. This is especially evident for TMSCl-quenched samples. To better understand this relationship; non-stoichiometric PhLi:**I**, reactions were run at 0.5 and 3.0 equivalents of PhLi. At ratios of 0.5:1 and 1:1, nearly identical product distributions are found for TMSCl-quenched samples. At 3 PhLi equivalents (−78 °C), the main product while still only monofunctionalized is now **V**, where one diol subunit is displaced by an –OSiMe_3 unit as detailed above. Though the nature of the monosubstituted products differ, the ratio of products to starting materials changes only slightly and significant amounts of **I** and TMS-benzene are found in the ^{29}Si NMR (Figure S5). This further suggests that a very large excess of PhLi is needed to push the equilibrium toward monosubstituted products at −78 °C, whereas at room temperature this excess would result exclusively in the tetraphenylsilane derivative. The EI-MS is similar to that for 1:1 samples, see SI.

Given that Corriu et al. suggest that these types of reactions must take place through hexacoordinated intermediates, which may still be true at ambient; our ability to generate only monophenyl-substituted products strongly suggests that the primary reaction intermediates generated at low temperatures

Continued.

Rxn ratio	Structures	Observed MS (m/z)	^{29}Si NMR /ppm	Quenched	Conversion[a]/% (^{29}Si NMR)
1:1 PhLi:**I** (−78 °C, 6 h)	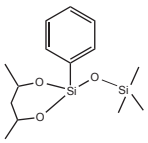	310.1	−65	Me_3SiCl	73 Ph*Si*(O)$_x$ 13 Ph_2**I**
	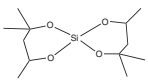	245.1 (M^+ − Me)	−82		
	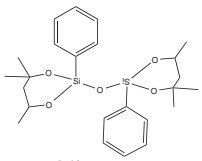 Oligomers	N/A	−66, −69		
	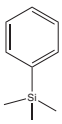	N/A	−4.8		
	$C_{15}H_{25}O_6Si_2$	357.1	ca. −66		
3:1 PhLi:**I** (−78 °C, 3 h)	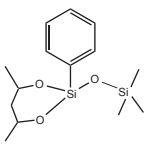	310.1	−65	Me_3SiCl	68 Ph*Si*(O)$_x$ 8 Ph_2**I**
	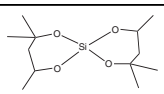	245.1 (M^+ − Me)	−82		
	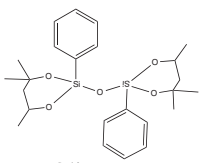 Oligomers	N/A	−65, −69		
	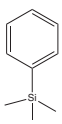	N/A	−4.8		
	$C_{15}H_{25}O_6Si_2$	357.1	ca. −66		
	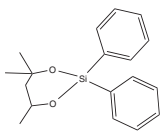	N/A	ca. −32		

a) Percent conversion calculated by ^{29}Si NMR integration ratio of product over total alkoxysilane present.

are pentacoordinated. Reactions run at −60, −40, 0, and 20 °C. Those run at ≤−40 °C gave monophenyl products at different reaction times, whereas warmer temperatures gave, tetraphenyl- or triphenylalkoxysilanes.

Hence it is clear that two mechanisms are operating. Given that it appears difficult to form large amounts of even the monosubstituted species, without using a large excess of the nucleophile, it is likely that polysubstituted species arise from disproportation rather than sequential addition. The latter mechanism should happen easily in the presence of excess nucleophile. This proposition is significantly different from what Corriu et al. have argued in the past. *It also greatly affects the product distribution achievable in simple nucleophilic reactions*.

Other Nucleophiles. Based on our desire to generate novel silsesquioxanes, we sought to extend these mechanistic studies to other nucleophiles, including: MeLi, *n*-butylLi, 3-pyridinylLi, Li-TMS-acetylide, Li-acetylide (ethylenediamine complex), thianaphthenylLi, 2-thienylLi, Li-phenylacetylide, 9-anthracenylLi, 9,9-dimethylfluorenylLi, and Me-naphthalenylLi. Trial reactions were run with 1.2:1 RLi:**I** stoichiometry,

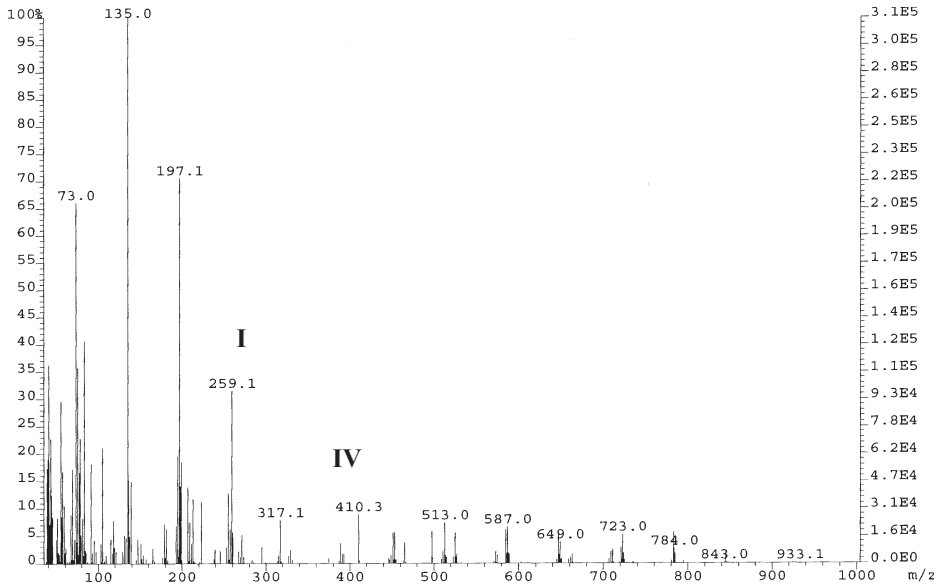

Figure 5. EI-MS of 1:1 PhLi:**I** after quenching with TMSCl; peaks: 410.3 m/z is **IV**, 259.1 is **I**.

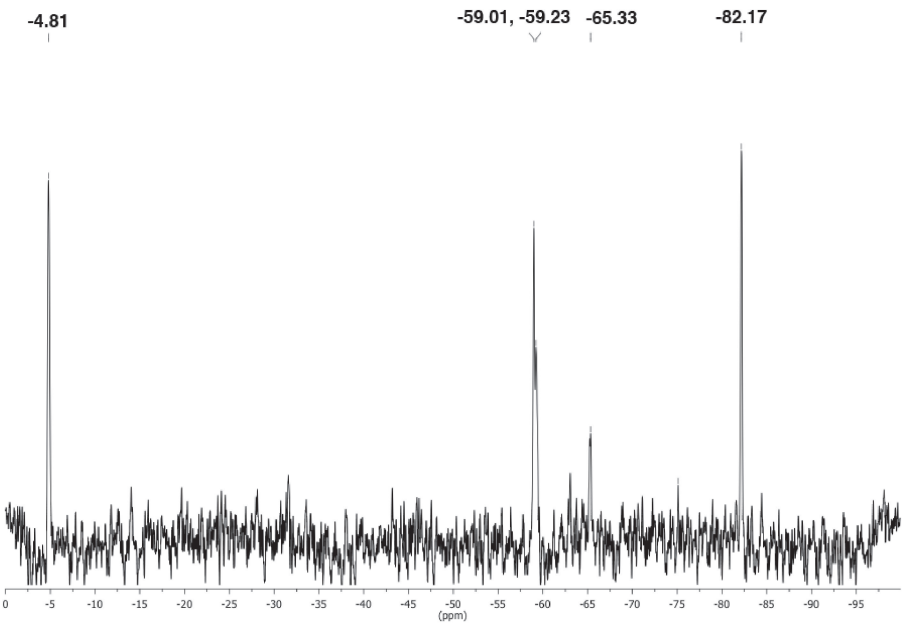

Figure 6. ^{29}Si NMR spectrum of the TMSCl quenched −78 °C 1:1 PhLi:**I**. Peaks: −4.8 ppm, TMS-benzene; −59 ppm Ph*Si*$(RO)_3$; −65 ppm Ph–*Si*–$OSiMe_3(OR)_2$.

are un-optimized and are in support of the utility of these reactions. The first five [MeLi, *n*-butylLi, 3-pyridinylLi, Li-TMS-acetylide, Li-acetylide (ethylenediamine complex)], do not provide observable/isolable monomeric products. Only starting material **I**, ROP by-products and TMS-substituted starting materials are observed by mass spectral analysis and/or ^{29}Si NMR. Grignard reagents were also explored; however either no reaction or unidentifiable products were observed likely resulting from formation of stable pentacoordinated complexes with **I**.[33,34]

In contrast, 2-thienylLi, Li-phenylacetylide, anthracenylLi, 9,9-dimethylfluorenylLi, and Me-naphthalenylLi all gave products that could be characterized by both ^{29}Si NMR and EI-MS (Table 3). Most reactions were run using methods akin to those of Manoso et al.,[10] Jung et al.,[11] and those for PhLi above, in which an arylbromide is first converted to a lithium reagent via exchange with *n*-butylLi, followed by addition of **I** (structures **VIII**–**X**). The ^{29}Si NMR and EI-MS for each of these compounds are presented in SI, Figures S6–S12.

The nucleophilic reactions with the best conversions from **I** were (ca. 100%) for the anthracenylLi:**I** (Reaction 13) and Li-phenylacetylide:**I** reactions; no **I** remained in either case by ^{29}Si NMR. The 2-thienylLi:**I** (**VI**) shows ca. 18% conversion of **I** by ^{29}Si NMR and two types of products as discussed above for Ph**I** reactions (13.2, 6.2, −62 ppm), in which the TMS quenching group is either attached to the diol, or directly attached to the central Si atom (Si–O–TMS) (Table 3). The Li-phenylacetylide:**I** (**VII**) reaction with **I** at room temperature gives ca. 100% conversion by ^{29}Si NMR (−78 ppm), with no remaining spirosiloxane observed, and with product peaks in

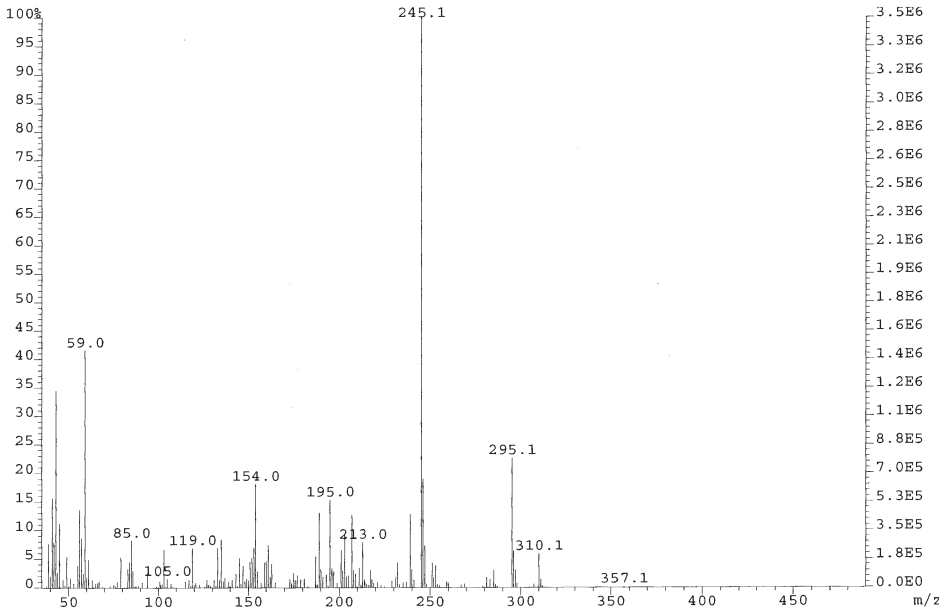

Figure 7. EI-MS of 1:1 PhLi:**I** (4.5 h, −78 °C), quenched with TMSCl; **I** − Me at 245.1 m/z, **V** at 310.1 m/z, and **V** − Me at 295.1 m/z.

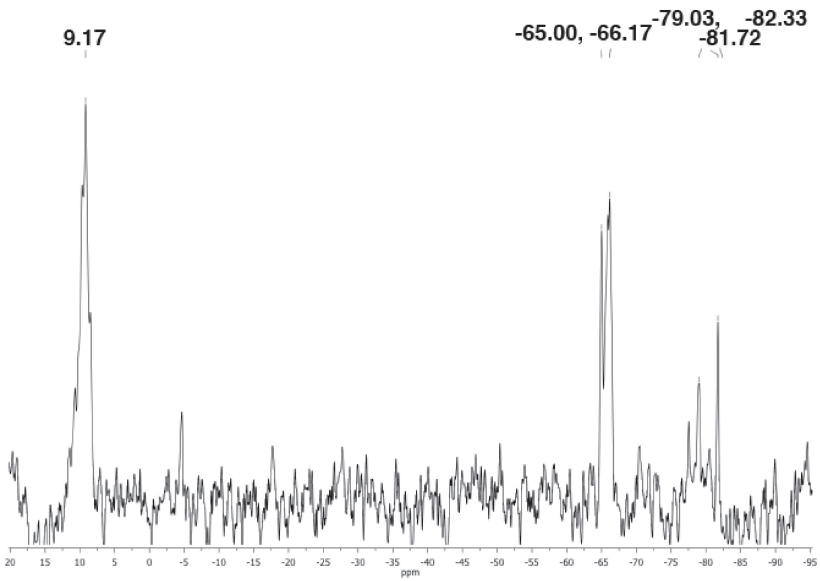

Figure 8. ^{29}Si NMR spectrum of 1:1 PhLi:**I** (4.5 h, −78 °C) quenched with TMSCl, Peaks ≈55–65 ppm are Ph$Si(O)_x$ units, peak at 9.17 ppm is Si–O–SiMe$_3$, peak at −82 ppm is **I**.

EI-MS at 334.0 and 434.1 m/z for the two monomeric structure types respectively (Table 3). The 9,9-dimethylfluorenyl-Li:**I** (**IX**) reaction shows ca. 15% conversion of **I** by ^{29}Si NMR (−52.6 and −65.0 ppm) and a clear peak in EI-MS at 426.1 m/z for an Si–O–TMS-structured monomeric product (Table 3).

Lastly, Me-naphthalenylLi:**I** (**X**) shows ca. 29% conversion of **I** to Me-naphthalenyl products by ^{29}Si NMR (−46.1, −57.5 ppm). The peak at −57.5 ppm corresponds to the expected structure formed by lithium–bromide exchange on 1-bromo-4-methylnaphthalene starting material, followed by direct attack of **I** (Table 1 for examples). The peak at −46.1 ppm, is attributed to the product from deprotonation of the methyl group by either *n*-butylLi or 4-methylnaphthalenylLi (due to its lower pK_a), and attack by the methylenylLi group on **I**. Alkyltrieth-oxysilanes typically give ^{29}Si NMR peaks in the −45 ppm region (Table 1). By EI-MS only one product mass is observed at 402.2 m/z. This peak could correspond to both products observed by ^{29}Si NMR since they would have the same molecular formula. Note also that the observed mass is for a proton-quenched derivative, instead of being quenched with TMS (Table 3). This transfer may occur during the aqueous workup used to remove salts or is a result from incomplete quenching.

As an example, Figure 9 shows the EI-MS for anthracenyl**I** (**VIII**) quenched with Me$_3$SiCl, with the product peak [M] at 410.2 m/z and [M − TMS] at 338.1 m/z. Figure 10 shows the ^{29}Si NMR of **VIII**, with the product peaks at 10.0 and −57.4 ppm, and TMS-anthracene at −2.87 ppm. Silsesquioxanes of **VIII** will be discussed in that section.

Table 3. Reaction conditions and observed characterization data for RLi reactions with **I**, all reactions were conducted at −78 °C for 3 h and quenched with Me_3SiCl unless otherwise noted

Rxn ratio/Conditions	Structure	Observed MS (m/z)	^{29}Si NMR /ppm	Conversion/% (^{29}Si NMR)
1.2:1 2-thienylLi:**I** (**VI**) 0 °C	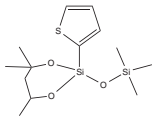	316.2	6.66, −62.58	18
	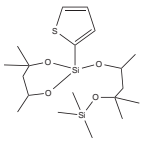	416.8	13.24, −62.06	
		156.3	−7.2	
	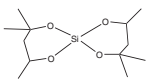	245.1 (M^+ − Me)	−82	
1.2:1 Li-phenylacetylide:**I** (**VII**) 25 °C	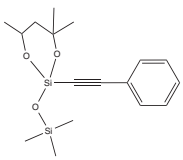	334.0	−78.8	100
	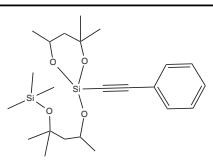	434.1	−78.3	
	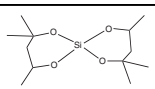	245.1 (M^+ − Me)	−82	
1.2:1 anthracenylLi:**I** (**VIII**)	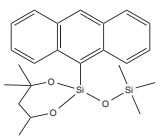	272.3	−53.4, 10.0	100
	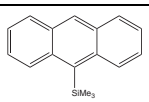	250.1	−2.9	
	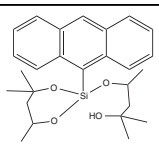	438.2	−53.9	

Continued on next page.

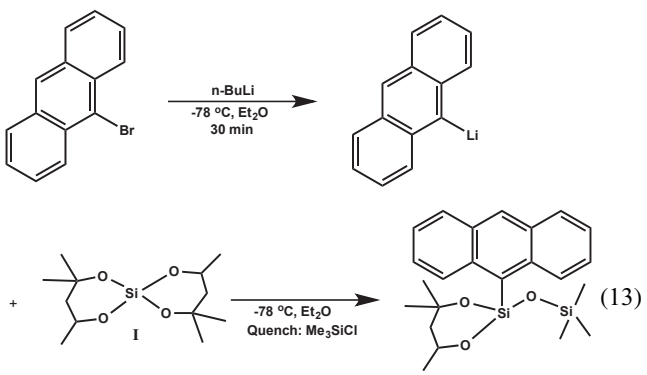

(13)

As with the Ph**I** derivatives, no simple method was found to isolate the monomeric products from **I**. For example bulb-to-bulb distillation attempts led to distillation of **I** and functionalized products simultaneously. Note this is also similarly observed in the distillation of **I** from diol.[24] Reactions that give low conversion also tend to show TMS-R by-products from quenching, likely due to equilibration between **I** and RLi as found with PhLi. Future work will look at developing effective separation techniques and/or optimizing reaction conditions to make separation unnecessary.

TEOS Systems. For comparative purposes, we also ran the same studies with $Si(OEt)_4$. These reactions gave slightly

Continued.

Rxn ratio/Conditions	Structure	Observed MS (m/z)	^{29}Si NMR /ppm	Conversion/% (^{29}Si NMR)
1.2:1 9,9-dimethylfluorenylLi:**I** (**IX**)	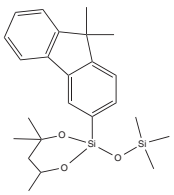	334.0	N/A	16
	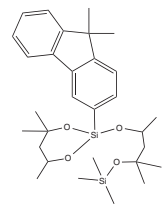	434.1	−52.6	
	Dimer/Oligomers	N/A	−65.8	
	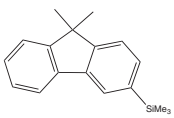	251.0 (M^+ − Me)	−4.8	
	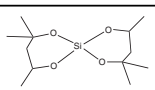	245.1 (M^+ − Me)	−82.4	
1.2:1 Me-naphthalenylLi:**I** (**X**)	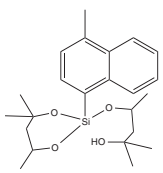	402.2	14.7, −57.5	23
	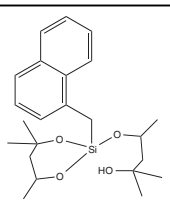	402.2	−46.1	
	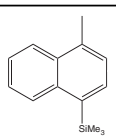	N/A	−5.8	
	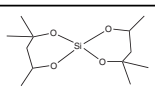	N/A	−82	

different product distributions also highly temperature dependent. For example, Ph:**I** reactions favor mono- or tetrafunctionalization with little di- or trifunctionalization regardless of starting material ratio at temperatures below −40 °C. Ph:TEOS reactions result in a mixture of mono- and difunctional products, with unreacted TEOS also remaining in 1:1 PhLi:TEOS systems at −78 °C. In general, reactions run at or below −40 °C favor mono- and difunctionality, reactions at 0 °C favor di- and trifunctionality, and temperatures above 0 °C favor tetraphenylsilane. As with Ph:**I**, Ph:TEOS reactions were quenched with MeI or TMSCl before warming per conditions listed in Table 4. Thus, a −78 °C 1:1 PhLi:$Si(OEt)_4$ reaction quenched with MeI after 4 h gives the EI-MS shown in Figure 11.

As seen in Figure 11, the $PhSi(OEt)_3$ parent ion appears at $m/z = 240$, $Ph_2Si(OEt)_2$ appears at $m/z = 272.3$ and $PhSi(OEt)_2$ at $m/z = 194$ after losing ethoxy and the peak at $m/z = 227$ corresponds to the diphenyl species missing an EtO group. Unfortunately, peak intensities in mass spectra do not permit quantification of the individual species. However, the ^{29}Si NMR provides a somewhat more accurate estimation of the species present. Thus, Figure 12 indicates that at −78 °C, at a 1:1 ratio of $Si(OEt)_4$:PhLi, the products are $PhSi(OEt)_3$ (−58 ppm), $Ph_2Si(OEt)_2$ (−32 ppm), and $Si(OEt)_4$ (−82 ppm). The diphenyl

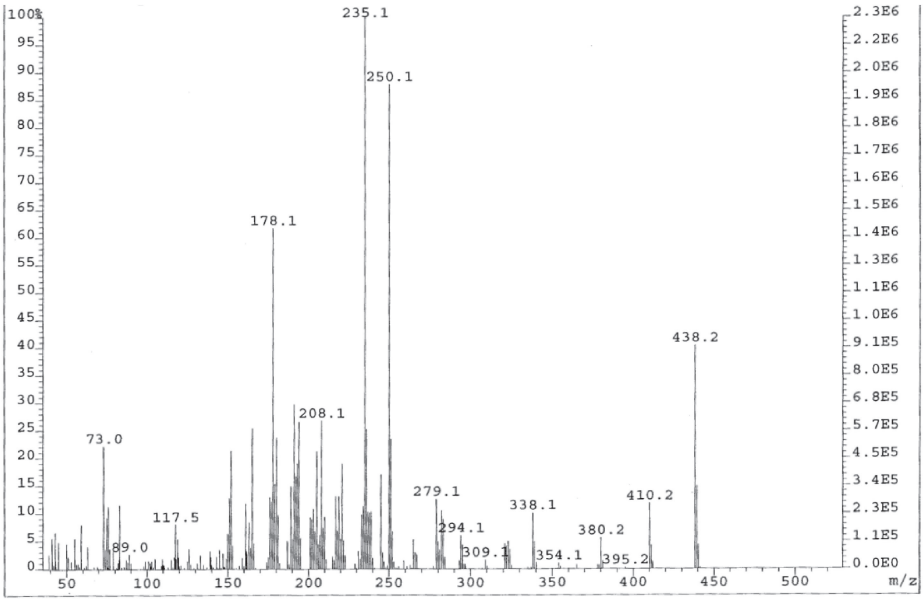

Figure 9. EI-MS of anthracenylLi:**I** (3 h, −78 °C), quenched with TMSCl; **VIII** at 410.2 m/z, **VIII** − Me at 395.2 m/z, **VIII** − TMS at 338.1 m/z, 438.2 is **VIII** + diol without TMS group.

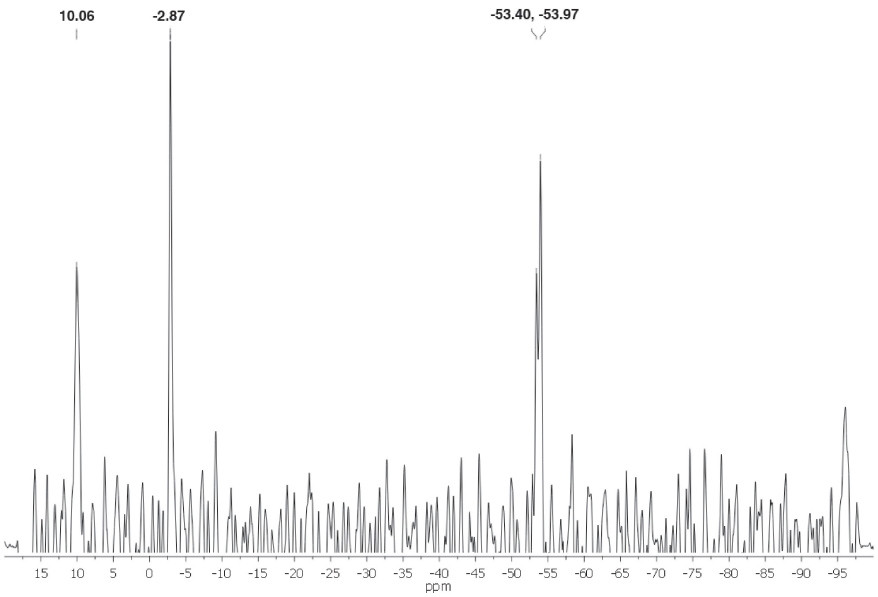

Figure 10. ^{29}Si NMR of 1:1 anthracenylLi:**I** (3 h, −78 °C, **VIII**) quenched with TMSCl, peak at 53.97 ppm is R–Si(OR)$_3$, peak at 53.40 is R–Si(OR)$_2$(OSiMe$_3$), peak at 10.06 ppm is Si–O–*Si*Me$_3$, peak at −2.87 is TMS-anthracene, **I** is unobserved at −82 ppm.

product seems to form in smaller amounts at this temperature compared to −40 °C, reinforcing the disproportionation mechanism. The ratio of species can be controlled to some degree. Thus, 0 °C favors formation of Ph_3SiOEt. At −78 °C/4 h quenching with MeI (30 min) or TMSCl gives similar results (Figures S13 and S14).

One might argue based on Corriu's work that we should not see any mono- or diphenyl products, yet that is all that is seen. However, Manoso et al.'s work suggests we might expect to see the monophenyl products. Note that Manoso et al. used excess $Si(OEt)_4$ at −78 °C as such, we also explored the use of excess alkoxysilanes discussed further below.

Figure S16 shows the EI spectrum of 0.5:1 PhLi:TEOS at −78 °C, with the peak at 240.1 m/z corresponding to PhSi(OEt)$_3$ and the peak at 208.1 m/z corresponding to unreacted TEOS. The peak heights suggest that the ratios are ≈1:1, which is expected for a 0.5:1 reaction of PhLi:TEOS. If this reaction is not quenched with MeI or TMSCl before warming up (Figure S17), the mass spectrum shows $Ph_2Si(OEt)_2$ at 272.3 m/z as the main phenyl product, as well as unreacted TEOS at 208 m/z. This shows the importance of quenching the reaction at low temperature before workup.

We also explored 0.6:1 PhLi:TEOS systems at −40 °C, the results of which are similar to those at −78 °C, but at a fraction of the reaction time (30 min vs. 4 h). We see $Ph_2Si(OEt)_2$:PhSi(OEt)$_3$:TEOS distributions similar to those for the 1:1

Table 4. Reaction conditions and observed characterization data for PhenylLi reactions with TEOS, all reactions were conducted at −78 or −40 °C for 30 min–2 h (TE: TEOS)

Rxn ratio/Conditions	Structures	Observed MS (m/z)	^{29}Si NMR /ppm	Quenched	Conversion/% (^{29}Si NMR)
1:1 Ph:TE (−78 °C)	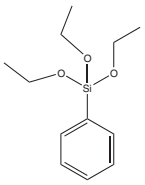	239.9	−57.9	MeI	45 $PhSi(OEt)_3$, 18 $Ph_2Si(OEt)_2$
	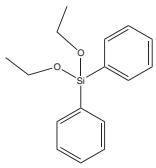	271.9	−32.2		
	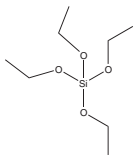	N/A	−81.6		
0.5:1 Ph:TE (−78 °C)	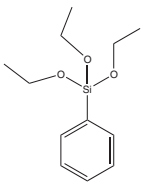	240.1	−57.9	MeI	34 $PhSi(OEt)_3$, 12 $Ph_2Si(OEt)_2$
	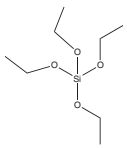	208.1	−81.6		
0.5:1 Ph:TE (−78 °C)	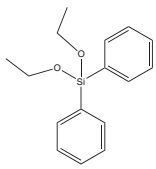	272.3	N/A	No	N/A
	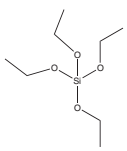	208.1			

Continued on next page.

reaction at −78 °C (Figure S18) in the ^{29}Si NMR spectra.

Furthermore, at 0.5:1 PhLi:TEOS at 0 °C we observe $Ph_3Si(OEt)$ as the dominant species by EI-MS (Figure S19). This is expected, as higher temperatures favor its formation, and since for the TEOS reactions once one phenyl reacts, the overall reactivity increases.

The most important observation is that even at low temperatures and sub-stoichiometric PhLi:TEOS ratios, the reaction products still contain $Ph_2Si(OEt)_2$ in considerable quantities, as found by Manoso et al.[10] These results seem to at least partially support a hexacoordinated silicon mechanism of nucleophilic attack. However, $PhSi(OEt)_3$ is still present so there likely exists an equilibrium between the three species as discussed for the Ph**I** samples (Ph_2:Ph:TEOS).

Summary of Findings. In these studies on nucleophilic substitution of **I** and TEOS, we find that reaction temperature, and low-temperature quenching are extremely important to achieve monosubstitution. However, contrary to previous studies, we find that **I** reacting with excess (3 equiv) RLi still generates monofunctional products. We also find that at low temperatures, monofunctional-alkoxysilanes form exclusively, and then on warming PhLi must transfer to the other monofunctional-alkoxysilanes and then to difunctional-alkoxysilanes, etc. until only Ph_4Si and **I** remain. This sug-

Continued.

Rxn ratio/Conditions	Structures	Observed MS (m/z)	^{29}Si NMR /ppm	Quenched	Conversion/% (^{29}Si NMR)
0.6:1 Ph:TE (−40 °C)	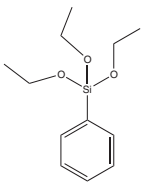	240.1	−58.7	Me_3SiCl	26 $PhSi(OEt)_3$, 18 $Ph_2Si(OEt)_2$
	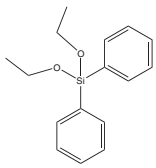	N/A	−32.8		
	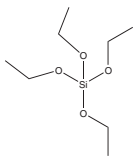	208.1	−82.4		
1:1 Ph:TE (−78 °C)	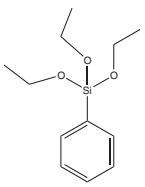	240.1	−58.7	Me_3SiCl	49 $PhSi(OEt)_3$, 15 $Ph_2Si(OEt)_2$
	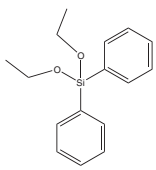	N/A	−32.8		
	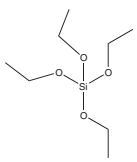	208.1	−82.4		

gests that temperature influences the nature of attack on **I**; at <−40 °C unsubstituted **I** is most reactive and forms a stable pentacoordinated intermediate, and at >−40 °C R-**I** is most reactive toward nucleophilic attack suggesting that disproportionation occurs much more readily.

Silsesquioxane (SQ) Synthesis. To verify the utility of the materials made by nucleophilic substitution of **I**, we explored the synthesis of phenylSQs, anthracenylSQs, and 9,9-dimethylfluoreneSQs (Reaction 14). The first step was to learn to purify the products. **I** and **IV** can be recovered in a mixture after vacuum distillation, but are very difficult to separate further. However, if the 1:1 PhLi:**I** reaction is run longer than 3 h/−78 °C then oligomeric materials result that do not distill. Treating these oligomeric materials with catalytic TBAF (see Experimental) provides cage compounds.[21,22] Thus GPC (Figure 13) and MALDI-TOF (Figure 14) analyses verify the formation of a mixture of $PhT_{8,10,12}$ and some partial cages, which could be separated by selective solubility.

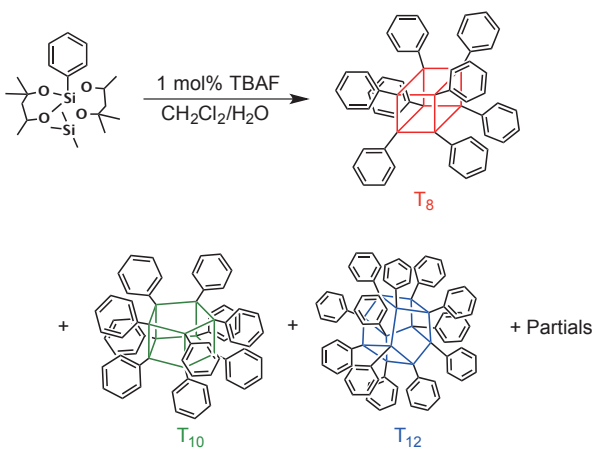

(14)[22]

Anthracenyl**SQ**s and 9,9-dimethylfluorene**SQ**s were made by the same method described for phenyl**SQ**s. These are

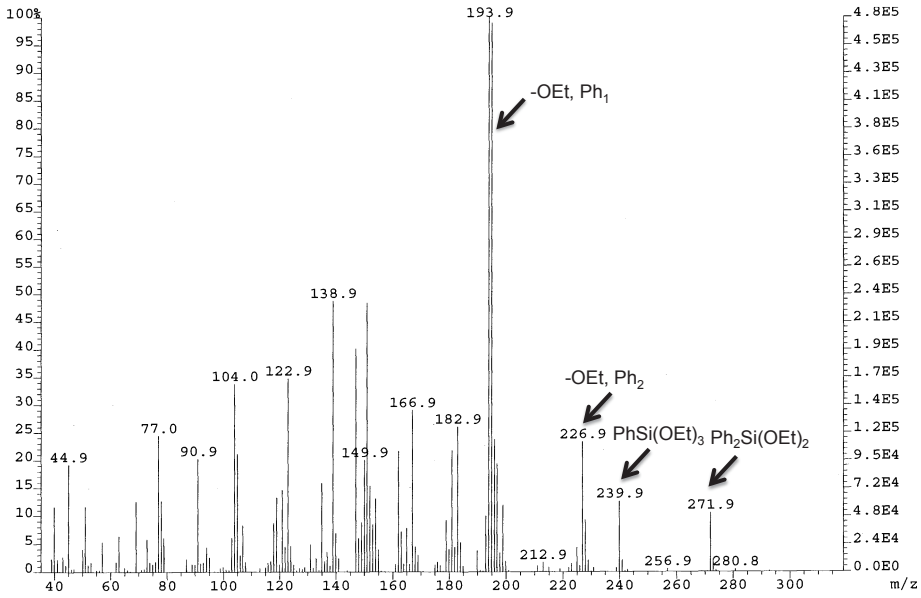

Figure 11. EI-MS of 1:1 PhLi:TEOS after quenching with MeI at −78 °C.

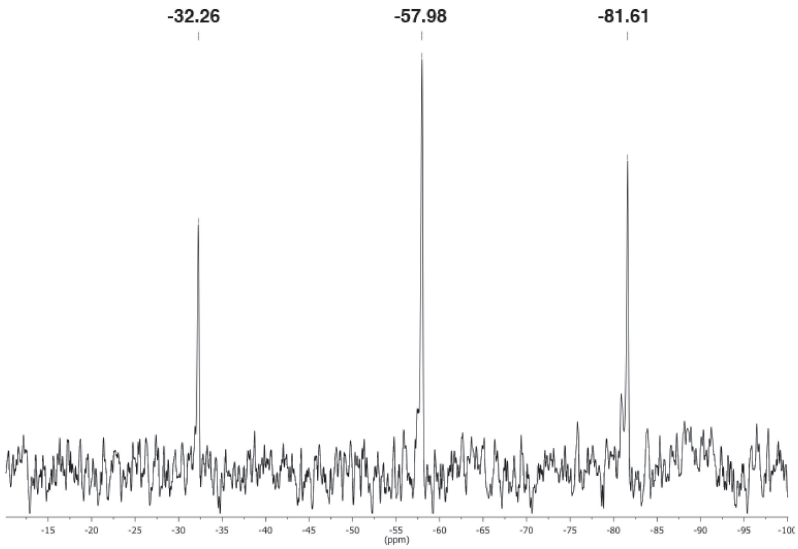

Figure 12. ^{29}Si NMR of 1:1 Ph:TEOS, −32.2 (18% Ph_2TE), −57.9 (Ph_1TE), −81.6 (TEOS) after quenching with MeI.

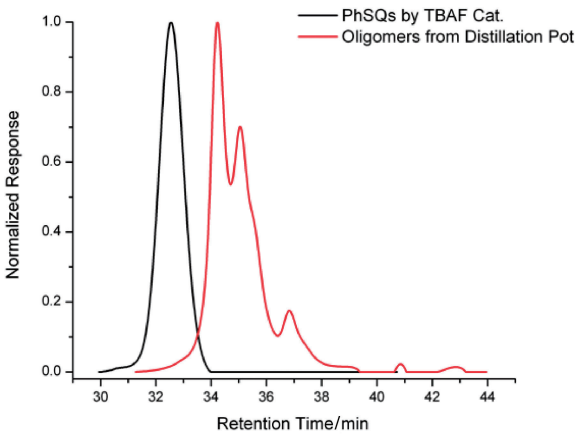

Figure 13. GPC trace comparison of oligomeric materials from 1:1 PhLi:**I** (6 h) compared with an overnight TBAF catalyzed PhSQ synthesis.

exciting systems since no known anthracenylSQs or 9,9-dimethylfluoreneSQs with direct attachment have been reported. The isolated cage yields were ca. 58 and 82% respectively. Figures 15 and 16 show the MALDI-TOF spectra of the anthraceneSQ and 9,9-dimethylfluoreneSQ cage mixtures respectively. Due to the large size of the anthracene and 9,9-dimethylfluorene substituents, the cage formation process results in many partial cages, with T_7 monohydroxide as the predominant structures in both cases. Note the formation of the TMS derivative as a by-product from the quenching process in the anthracene derivative (1525.6 m/z); alternative-quenching methods such as MeI would alleviate these by-products.

The synthesis of phenylacetyleneSQs is also explored since the monofunctional phenylacetylene**I** is easily made at RT. However, it proved difficult to make cages by F^--catalyzed rearrangement due to the sensitivity of the Si–C bond and its

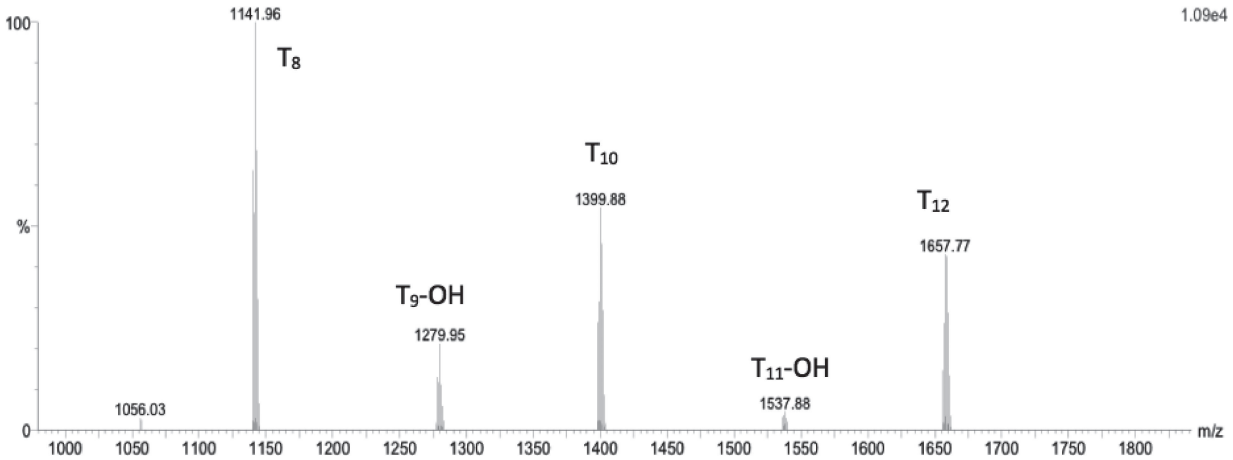

Figure 14. MALDI-TOF spectrum of PhSQs made by TBAF-catalyzed reaction of Ph**I** oligomers; all peaks are Ag^+ ions.

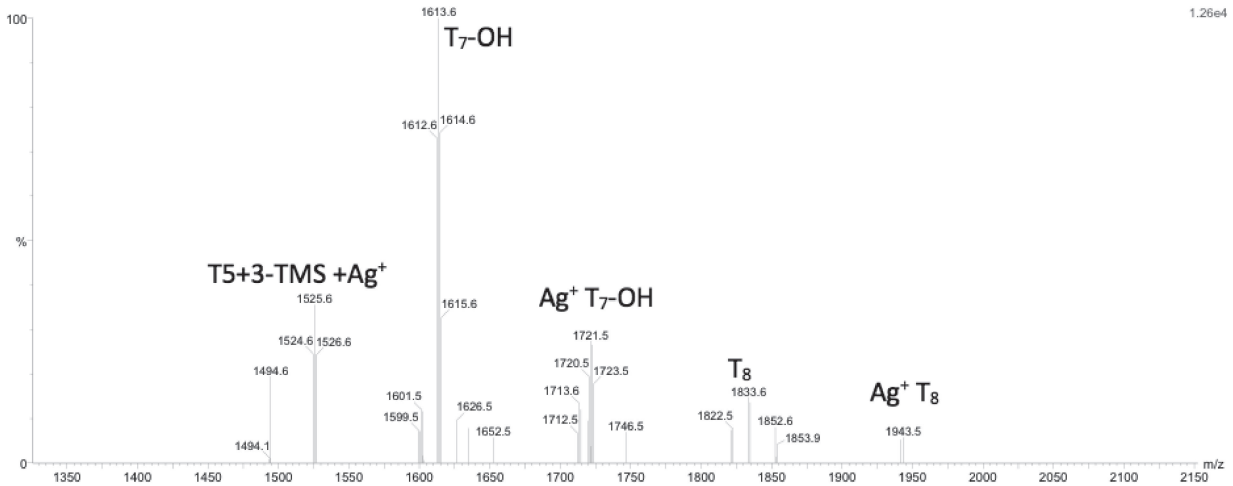

Figure 15. MALDI-TOF spectrum of anthraceneSQs made by TBAF-catalyzed reaction of anthracenyl**I** (**VIII**).

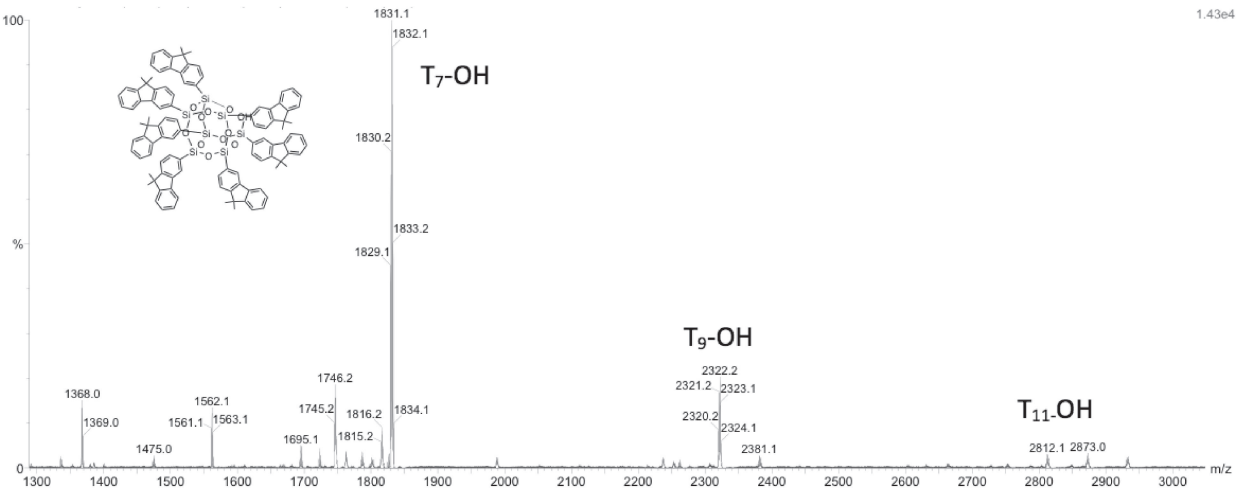

Figure 16. MALDI-TOF spectrum of 9,9-dimethylfluoreneSQs made by TBAF-catalyzed reaction of 9,9-dimethylfluorene**I** (**IX**), all peaks are Ag^+ ions.

propensity to undergo F^--catalyzed cleavage (deprotection) destroying the starting material and resulting in precipitated silica as a by-product. At 0 °C it was possible to obtain a very low yield <ca. 2% of the T_9-$(OH)_3$ derivative. Other methods of cage formation including acid catalysis were unsuccessful in generating the desired SQ products.

AnthracenylSQs and 9,9-dimethylfluoreneSQs are new compounds with potentially interesting photophysical proper-

ties even though the cages are incompletely condensed.[35] We explored the absorption and emission behavior (Figures S24 and S25). For anthracenylSQ the absorption and emission show maxima at 371 and 422 nm, and are both red-shifted from the parent anthracene by 10 and 25 nm respectively.[36] For 9,9-dimethylfluoreneSQs the absorption and emission maxima are at 268 and 322 nm, each shifted by ca. 7 nm.[37,38] The parent phenylacetylene shows absorption and emission peaks at 235 and 248 nm. To the contrary, phenylacetyleneSQ (Figure S26) absorption and emission peaks are present at 284/366 and 427 nm respectively, suggesting further conjugation and/or excimer formation once attached to the cage. These and other exciting new cage systems derived from these studies will be explored in the future.

Conclusion

We have illustrated an important development in siloxane chemistry, in which we can go from a biosourced silica (RHA) to functional alkoxysilanes. Our method uses RLi nucleophiles at low temperatures to functionalize spirosiloxanes made from RHA, which when quenched with an electrophile such as MeI or Me_3SiCl give mono-R-alkoxysilanes; and unquenched give tetra-R-silanes with reasonable conversions. We propose that the mechanism of nucleophilic substitution takes place through a pentacoordinate intermediate below −40 °C, which if unquenched and warmed to room temperature is capable of transferring PhLi. We find that aryl halides can be easily converted to Li reagents, which can then undergo nucleophilic substitution on spirosiloxanes, while alkylLi reagents and Grignard reagents do not give clear substitution. Alkynyl derivatives such as phenylacetylene also show clean substitution with ca. 100% conversion of the spirosiloxane to a monofunctional derivative. We have further demonstrated that silsesquioxanes can be made from monofunctional spirosiloxanes, with a never before observed anthraceneSQ.

With this class of materials, we can envision making new functionalized silsesquioxanes directly from most any arylhalide, as well as the possibility for other hybrid polymeric materials. Control to achieve disubstituted (mono- and difunctional) materials selectively can also be imagined for making new classes of siloxane polymers, all this while avoiding the use of chlorosilanes.

The authors would like to thank Intel Corporation through MSR-Task 2170.001 for partial support of this work. We would also like to thank the University of Michigan Rackham Graduate School for a Predoctoral Fellowship. We would also like to thank Mayaterials Inc. for starting materials for **I** synthesis. We would like to thank Clemens Krempner for a fruitful discussion about the failure of Grignard reactions due to complexation in these studies. Lastly, we would like to thank James Windak and Paul Lennon in the UM Mass Spec lab for all their help.

Supporting Information

Additional characterization including, Mass Spectrometry, NMR, and FTIR for synthesized compounds are included in the supporting information. This material is available on http://dx.doi.org/10.1246/bcsj.20160039.

References

1 E. G. Rochow, *J. Am. Chem. Soc.* **1945**, *67*, 963.
2 W. H. Daudt, Production of Phenyltrichlorosilane, U.S. Patent 2,576,448, Nov. 27, **1951**.
3 T. J. Barton, P. Boudjouk, *Organosilicon Chemistry: A Brief Overview*, in *Silicon-Based Polymer Science*, in *Advances in Chemistry*, **1989**, Vol. 224, Chap. 1, pp. 3–46. doi:10.1021/ba-1990-0224.ch001.
4 *The Chemistry of Organic Silicon Compounds*, ed. by Z. Rappoport Y. Apeloig, John Wiley & Sons Ltd., London, **1998**, Parts 1–3.
5 E. T. McBee, C. W. Roberts, G. F. Judd, T. S. Chao, *J. Am. Chem. Soc.* **1955**, *77*, 1292.
6 P. D. George, L. H. Sommer, F. C. Whitmore, *J. Am. Chem. Soc.* **1955**, *77*, 6647.
7 J. M. Tour, J. A. John, E. B. Stephens, *J. Organomet. Chem.* **1992**, *429*, 301.
8 G. Silverman, P. Rakita, *Handbook of Grignard Reagents*, Marcel Dekker, **1996**, pp. 667–675. doi:10.1201/b16932-33.
9 B. A. Klokov, *Org. Proc. Res. Dev.* **2001**, *5*, 234.
10 A. S. Manoso, C. Ahn, A. Soheili, C. J. Handy, R. Correia, W. M. Seganish, P. DeShong, *J. Org. Chem.* **2004**, *69*, 8305.
11 K.-H. Jung, S.-Y. Kim, W. Tan, D.-S. Shin, C. Ahn, *Bull. Inst. Basic Sci.* **2005**, *17*, 79.
12 A. Boudin, G. Cerveau, C. Chuit, R. J. P. Corriu, C. Reye, *Angew. Chem., Int. Ed. Engl.* **1986**, *25*, 474.
13 A. Boudin, G. Cerveau, C. Chuit, R. J. P. Corriu, C. Reye, *Angew. Chem., Int. Ed. Engl.* **1986**, *25*, 473.
14 A. Boudin, G. Cerveau, C. Chuit, R. J. P. Corriu, C. Reye, *Organometallics* **1988**, *7*, 1165.
15 R. J. P. Corriu, J. C. Young, in *Chemistry of Organic Silicon Compounds*, ed. by S. Patai, Z. Rappaport, Wiley, Chichester, **1989**, Chap. 20. doi:10.1002/0470025107.ch20.
16 R. Corriu, *Pure Appl. Chem.* **1988**, *60*, 99.
17 R. M. Laine, M. F. Roll, *Macromolecules* **2011**, *44*, 1073.
18 J. C. Furgal, J. H. Jung, T. Goodson, III, R. M. Laine, *J. Am. Chem. Soc.* **2013**, *135*, 12259.
19 J. H. Jung, R. M. Laine, *Macromolecules* **2011**, *44*, 7263.
20 J. H. Jung, J. C. Furgal, T. Goodson, III, T. Mizumo, M. Schwartz, K. Chou, J.-F. Vonet, R. M. Laine, *Chem. Mater.* **2012**, *24*, 1883.
21 J. C. Furgal, T. Goodson, III, R. M. Laine, *Dalton Trans.* **2016**, *45*, 1025.
22 J. C. Furgal, J. H. Jung, S. Clark, T. Goodson, III, R. M. Laine, *Macromolecules* **2013**, *46*, 7591.
23 R. M. Laine, K. Y. Blohowiak, T. R. Robinson, M. L. Hoppe, P. Nardi, J. Kampf, J. Uhm, *Nature* **1991**, *353*, 642.
24 R. M. Laine, J. C. Furgal, P. Doan, D. Pan, V. Popova, X. Zhang, *Angew. Chem., Int. Ed.* **2016**, *55*, 1065.
25 N.-D. Chuy, V. Chvalovský, J. Schraml, M. Mägi, E. Lippmaa, *Collect. Czech. Chem. Commun.* **1975**, *40*, 875.
26 F. Carre, C. Chuit, R. J. P. Corriu, A. Fanta, A. Mehdi, C. Reye, *Organometallics* **1995**, *14*, 194.
27 N. Kano, N. Nakagawa, T. Kawashima, *Angew. Chem., Int. Ed.* **2001**, *40*, 3450.
28 Y. Sugahara, T. Inoue, K. Kuroda, *J. Mater. Chem.* **1997**, *7*, 53.
29 T. Jermouni, M. Smaihi, N. Hovnanian, *J. Mater. Chem.* **1995**, *5*, 1203.

30 E. Liepiņš, I. Zicmane, E. Lukevics, *J. Organomet. Chem.* **1986**, *306*, 167.
31 A. K. Bhattacharya, G. Thyagarajan, *Chem. Rev.* **1981**, *81*, 415.
32 a) S.-G. Kim, S. Sulaiman, D. Fargier, R. M. Laine, Simple Syntheses of Octaphenyloctasilsesquioxane and Polyphenylsilsesquioxane. Starting Point for Aromatic Nanocomposites with Complete Control of Physical and Chemical Properties at Nanometer Length Scales, in *Materials Syntheses: A Practical Guide*, ed. by U. Schubert, N. Hüsing, R. Laine, Springer-Verlag, Weinheim, **2008**, pp. 179–182. doi:10.1007/978-3-211-75125-1_24. b) R. M. Laine, unpublished work.
33 A. L. Spek, P. Voorbergen, G. Schat, C. Blomberg, F. Bickelhaupt, *J. Organomet. Chem.* **1974**, *77*, 147.
34 E. C. Ashby, M. B. Smith, *J. Am. Chem. Soc.* **1964**, *86*, 4363.
35 Y. Chujo, K. Tanaka, *Bull. Chem. Soc. Jpn.* **2015**, *88*, 633.
36 C. A. Parker, W. T. Rees, *Analyst* **1960**, *85*, 587.
37 H. Qi, J. Chang, S. H. Abdelwahed, K. Thakur, R. Rathore, A. J. Bard, *J. Am. Chem. Soc.* **2012**, *134*, 16265.
38 R. G. Harvey, P. P. Fu, P. W. Rabideau, *J. Org. Chem.* **1976**, *41*, 2706.

